land

MDPI

Article

Using Different Extraction Methods to Estimate Soil Salinity and Salt Type Changes and Their Effects on Soil Inorganic Carbon in Plowed Desert–Sierozem Soil

Kang Peng [1,2], Fang Zhang [1,2,*] and Zhidong Shao [1,2]

[1] College of Geography and Remote Sensing Sciences, Xinjiang University, Urumqi 830017, China; pkang@stu.xju.edu.cn (K.P.); 107552101037@stu.xju.edu.cn (Z.S.)
[2] Xinjiang Key Laboratory of Oasis Ecology, Xinjiang University, Urumqi 830017, China
* Correspondence: zhangfang@xju.edu.cn; Tel.: +86-139-9929-7925

Abstract: Understanding the actual soil salt ion content and salt type is one of the important prerequisites for determining the nature of saline soils and their development and utilization in drylands. Desert–sierozem soils are widely distributed in the plains between the northern piedmont of the Tianshan Mountains and the Gurbantunggut Desert in Xinjiang, Northwest China, which contain abundant calcium sulfate (gypsum) and calcium carbonate and are high-quality arable land resources for agriculture. These soils have been extensively reclaimed for farmland in recent decades. In this study, 10 plots of desert–sierozem soils with different tillage years in the Qitai Oasis plain area in the northern piedmont of Tianshan Mountain were studied. Three soil profiles were excavated in each sample plot with a depth of 1.2 m. A total of 30 farmland profiles were dug up and sampling was conducted according to the soil occurrence layers of the farmland. All the soil samples were predominantly sandy in texture, with more than 92% of the soil particles distributed between 0.05 and 0.25 mm, and less than 8% between 0.002 and 0.05 mm. Conventional water extraction (CWE) and intensified water extraction (IWE) were adopted to extract the water-soluble salt ions content of K^+, Na^+, Ca^{2+}, Mg^{2+}, Cl^-, $SO_4{}^{2-}$, $HCO_3{}^-$ and $CO_3{}^{2-}$, and this study compared the extraction results using two different methods with varying extraction strengths. Additionally, the calcium sulfate and calcium carbonate contents were obtained using the chemical extraction and mineral assay methods, respectively. Differences in the salts and salt types in desert–sierozem soils with different tillage years were analyzed, and the effect of calcium sulfate on the inorganic carbon sinks in plowed desert–sierozem soil was demonstrated. The findings indicated that the standard conventional extraction procedure involving a 5:1 water–soil ratio and 3 min of shaking was inadequate for accurately measuring the soil salt content in high calcium sulfate content desert–sierozem soils. With the IWE method, by increasing the water–soil ratio, prolonging the shaking time, and grinding the particles finer, the amount of water-soluble salts extracted using the IWE method was 5.83 times higher than that of the conventional method. Among them, the average content of IWE-Mg^{2+} increased by 123.41 mg kg^{-1} compared to CWE-Mg^{2+}, the average content of IWE-Ca^{2+} was 3.82 times higher than CWE-Ca^{2+}, with an average increase of 2931.59 mg kg^{-1}, and the IWE-$SO_4{}^{2-}$ content was 5.96 times higher than CWE-$SO_4{}^{2-}$, with an average increase of 8658.95 mg kg^{-1}. A markedly negative correlation ($p < 0.01$) was observed between calcium carbonate and calcium sulfate in desert–sierozem soils after tillage. The calcium sulfate content consistently decreased and calcium carbonate increased with an increasing number of tillage years. The pedogenic calcium carbonate content in desert–sierozem soils increased by an average of 10.86 g kg^{-1} after more than 40 years of cultivation, and the transfer of Ca^{2+} from calcium sulfate to calcium carbonate was identified as the cause of the increase in the soil inorganic carbon sink. Overall, a new method for extracting water-soluble salts was utilized for aridisols, which commonly consist of complex salt types. The results elucidate the changes in salinity within plowed desert–sierozem soils as well as the impact of soil salt on soil inorganic carbon sinks. Based on our research, desert–sierozem soils are well suited for agricultural farming because they contain high levels of sulfate, which is one of the important inorganic nutrients essential for crops, and it also provides a source of calcium for increasing inorganic carbon sinks. This study serves as a reference and scientific basis for soil carbon cycles in arid zones.

check for updates

Citation: Peng, K.; Zhang, F.; Shao, Z. Using Different Extraction Methods to Estimate Soil Salinity and Salt Type Changes and Their Effects on Soil Inorganic Carbon in Plowed Desert–Sierozem Soil. *Land* **2024**, *13*, 257. https://doi.org/10.3390/land13020257

Academic Editor: Amrakh I. Mamedov

Received: 8 January 2024
Revised: 16 February 2024
Accepted: 17 February 2024
Published: 19 February 2024

Copyright: © 2024 by the authors. Licensee MDPI, Basel, Switzerland. This article is an open access article distributed under the terms and conditions of the Creative Commons Attribution (CC BY) license (https://creativecommons.org/licenses/by/4.0/).

Keywords: Xinjiang desert–sierozem soils; extraction methods; water-soluble salt ions; calcium sulphate; calcium carbonate; soil inorganic carbon

1. Introduction

Most soils in arid zones belong to the aridisol category because of the limited precipitation and high evaporation. Xinjiang, the largest arid region in China, has predominantly desalinized base-stage soils because of its dry and cold conditions [1]. Therefore, these soils are typically rich in various combinations of salt types. For instance, saline soils accumulate soluble salts, particularly chloride salts, in their surface layers. Desert soils contain a layer of calcium sulfate (gypsum). Calcic aridisols feature a calcium-carbonate-enriched layer. Different salts exhibit different water solubilities. Chloride salts have higher solubility than those of calcium sulfate and calcium carbonate; in contrast, calcium sulfate dissolves more easily than calcium carbonate, and can be categorized as easily soluble, moderately soluble, and insoluble salts. In Xinjiang, there is a zonal soil called desert–sierozem soil that developed from the loess-like parent material of the pre-mountain plains located on the northern piedmont of the Tianshan Mountains. This alkaline soil combines the qualities of desert soil and sierozem and has a soil body rich in both calcium sulfate and calcium carbonate.

The parent material conditions of desert–sierozem soils are highly conducive to agriculture. The soil is deep, easy to cultivate, and of high value to the agricultural industry [2,3]. The Qitai Oasis, located in the northern piedmont of the Tianshan Mountains, experienced significant agricultural development between 1976 and 2016. During this period, the agricultural land area in the desert–sierozem soil region increased considerably from 3.25% to 40.80% [4]. The soil salinity content and characteristics directly affect crop growth, soil carbon sequestration, and ecosystem security [5–7]. The salinity in the profiles of desert–sierozem soils varies greatly during irrigated maturation, and farmed desert-sierozem soils show a reverse soil salinity succession process, i.e., the salts in the soils gradually decrease with an increasing duration of cultivation [8]. It was found that the longer the cultivation period, the more significant the reverse change in soil salinity, and the earlier the farmland is removed from the influence of the groundwater table, the earlier the reverse salinity succession process occurs and the more complete the soil desalination is [9]. Carbon fixed by carbonates in soil (mainly calcium carbonate) is also known as SIC (soil inorganic carbon), and the SIC content in arid zones is much higher than that of soil organic carbon [10–12]. Soil salinity is closely related to SIC, and an increasing number of studies have shown that soil salinity decreases with increasing SIC content [7,13,14]. It has been indicated that the higher the salinity of desert oasis farmland soils in arid zones, the higher the total amount of SIC obtained from the infiltration process [15]. In addition, in alkaline calcium-rich arid regions, the main pathway of carbon cycling is through atmosphere–vegetation–soil–water–SIC (mainly calcium carbonate) precipitation [16–18].

The methods for measuring soil salinity were also different in different regions [19–21]. Ismayilov et al. [21] analyzed salinity soil in the Kur-Araz basin in Azerbaijan by passing soil samples through a 2 mm sieve and setting a 5:1 water–soil ratio to make a suspension, and then oscillating the suspension for a total of four times, once every 30 min, for 1 min each time. Next, the suspensions were left for 4 h for filtering and extracting, and finally, the extracted data were used to evaluate the relationship between the EC and salt content of eight soil salinity types. At present, in Xinjiang, soil samples are usually collected using the conventional extraction method of passing through a 2 mm sieve, configuring the leaching solution with a 5:1 water–soil ratio, shaking for 3 min, and then filtering to obtain data on the soil water-soluble salts or salt ions [22–24], which are mainly used for saline soil research, especially for assessing the degree of soil salinization. Compared to saline soils, there are fewer studies on soil salinity and salt analyses in other aridisol types. The salts in the aridisols of Xinjiang mainly include chloride, sulfate, and carbonate–bicarbonate salts. Most of these soil salts consist of four cations (K^+, Na^+, Ca^{2+}, and Mg^{2+}) and four

anions (Cl^-, SO_4^{2-}, HCO_3^-, and CO_3^{2-}). Therefore, the salts in Xinjiang soils have been investigated in salinity studies [25,26], and the sum of the eight water-soluble salt ions (i.e., K^+, Na^+, Ca^{2+}, Mg^{2+}, Cl^-, SO_4^{2-}, HCO_3^-, and CO_3^{2-}) has often been used to express the total salt content of the soil, as it is very close to the true salt content obtained by the residue-drying mass method, with a relative error of ±10% or less [27].

Different salts reflect the different forms of elements in the soil, which are an important basis for studying the regularity of the migration, transformation, and cycling of elements [28,29]. Due to the complexity of the soil components, it is difficult to strictly determine the presence of elements in the soil in practice, and methods with different extraction capacities are usually used to determine the forms of the elements [30]. Based on Tessier's five-step method [31], the sequential extraction scheme of the European Community Bureau of Reference (BCR sequential extraction procedure) is a relatively mature scheme for the extraction of elemental forms from soil and sediment, and it has been applied to the extraction of elements in sediments [32,33], soils [34,35], dust [36] and sewage sludge samples [37]. It has been extensively studied, mainly for the extraction of heavy metal elements, and has also been used for the extraction of constant elements, such as K, Na, Ca, Mg, Fe, Mn, etc. [38]. The Chinese national standard GB/T 25282-2010 [39] was developed based on the BCR sequential extraction method with the addition of a water-soluble state extraction operation. Using this method, soil samples are finely passed through a 0.097 mm sieve and then continuously oscillated for 16 h at a 20:1 water–soil ratio. The extraction intensity of the elements is much higher than that of the conventional soluble salt extraction specification of passing through a 2 mm sieve and then oscillating for 3 min at a water–soil ratio of 5:1 [24,40,41].

Large areas of saline soils in Xinjiang have been extensively reclaimed as farmland. Because of the various salt types and high salinity, the conventional method (5:1 water–soil ratio, shaking for 3 min) may lead to the inadequate extraction of soil salts, which is detrimental to the accurate assessment of soil salinity and its impact on crop growth [42,43]. Therefore, the objective of this study was to determine the contents of eight water-soluble salt ions in desert–sierozem soils of different tillage years using the conventional water extraction (CWE) and intensified water extraction (IWE) methods, and the extraction results were compared and analyzed. In addition, SIC mainly exists in the form of $CaCO_3$ and itself is a kind of soil salt. Due to the low vegetation coverage, weak life activity process and lower soil organic carbon accumulation in arid/semi-arid areas, SIC can account for 90% of its total soil carbon pool [44], which is an indispensable part in the global carbon cycle and plays an important role in addressing climate change. Simultaneously, in this study, the contents of the medium-soluble salt calcium sulfate (gypsum) and the insoluble salt calcium carbonate (calcite) were also determined using chemical and crystalline mineralogical determination methods, respectively, to study the changes in salinity and salt types in desert–sierozem soils and their effects on SIC sinks after soil farming.

2. Materials and Methods

2.1. Study Area

The sampling area is located in the Qitai Oasis plain (44°2′–44°8′ N, 89°26′–89°48′ E) in the northern piedmont of the Tianshan Mountains in Xinjiang, Northwest China, which has a mid-temperate continental arid–semi-arid climate, with hot summers and cold winters. The average annual temperature is about 5.5 °C, the average annual precipitation is about 176 mm (rainfall is concentrated in the summer), evaporation reaches 2141 mm, and the frost-free period is 153 days. The locations of the sampling sites were distributed as shown in Figure 1, and all the crops were wheat. Irrigation water came from groundwater extracted from pumping wells with the same water quality, and the total dissolved salinity of the groundwater was 604.18 mg L^{-1}, which included $K^+ + Na^+$ content of 63.75 ± 2.55 mg L^{-1}, Ca^{2+} content of 81.36 ± 4.06 mg L^{-1}, Mg^{2+} content of 32.20 ± 2.65 mg L^{-1}, Cl^- content of 67.99 ± 1.92 mg L^{-1}, SO_4^{2-} content of 179.63 ± 3.74 mg L^{-1}, CO_3^{2-} content of 13.17 ± 0.44 mg L^{-1}, and HCO_3^- content of 166.08 ± 2.72 mg L^{-1}. The depth of the

groundwater was more than 10 m below the surface [45]; therefore, groundwater did not exert its effects on the sampling plot soil salinity by capillary force.

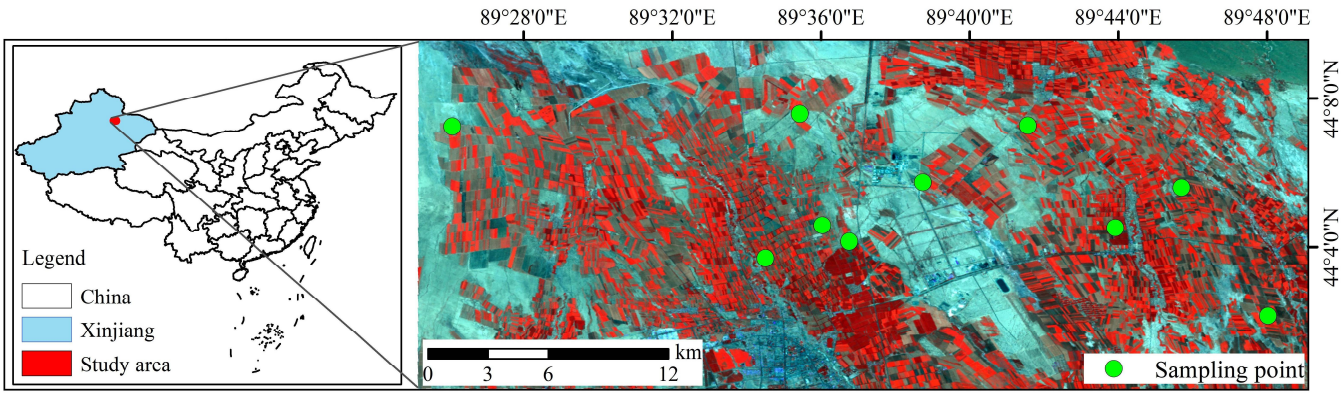

Figure 1. Location map of soils collected in the state of Qitai, Xinjiang.

2.2. Sample Collection and Preparation

Annual Landsat remote sensing images (https://www.gscloud.cn accessed on 2 July 2018) were used to prescreen sample plots from different cropping years. Field visits were conducted prior to sampling (to ensure consistency in the crop type, irrigation pattern, and fertilizer application) to determine the final sampling plots. The sample plots were all wheat plots, and the sample landscape is shown in Figure 2a. Sampling was conducted according to the soil occurrence layers of the farmland, as shown in Figure 2b, where soil samples were collected from the arable layer (A), plough subsoil layer (P), and subsoil layer (B). The soil in the plot was loess parent material, the soil cover was deep, with uniform color, and the accumulation of organic matter was not obvious but rich in carbonates. An obvious lime reaction was observed when 10% HCl was used during sampling, as shown in Figure 2c. After the soil samples were dried naturally, the roots and debris were removed, and the samples were ground using silica gel rods and a ceramic mortar, sieved, and prepared for measurement according to the following experimental specifications.

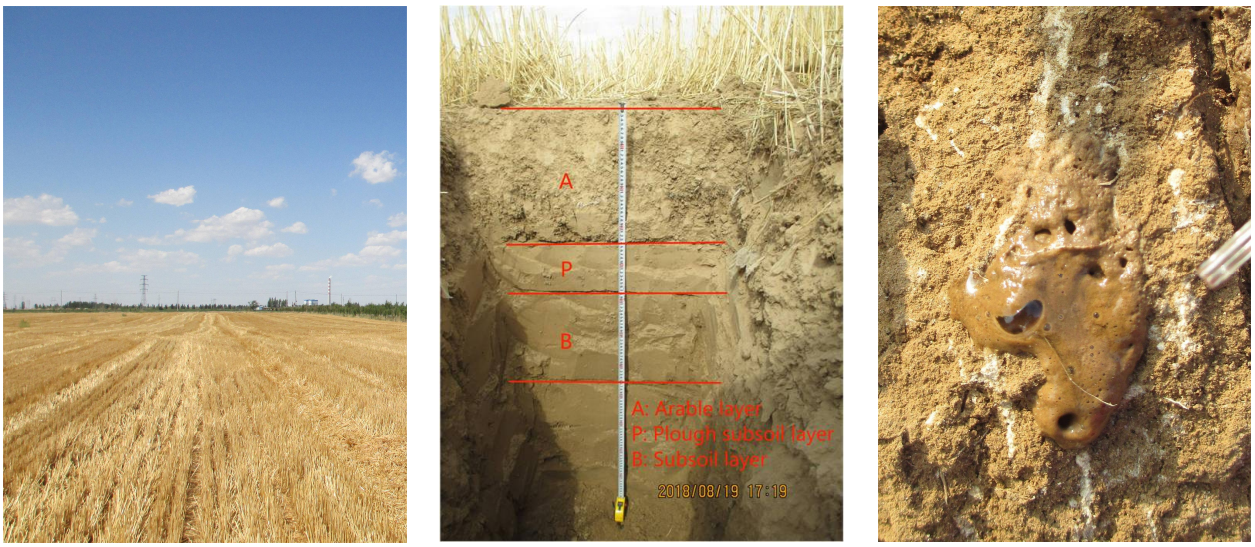

Figure 2. Characteristics of the sampled field and soil profile: (**a**) post-harvest wheat field; (**b**) soil profile; and (**c**) carbonate lime reaction.

2.3. Indicators and Methods

The two methods used for the extraction of water-soluble salt ions from soil are presented in Table 1. The standard material for composition analysis of the soil effective state, namely GBW07459a (ASA-8a), and blank test experiments were used for quality control, and each sample was analyzed in triplicate. All the reagents were chemically pure, and the water used in the experiments was ultrapure H_2O at pH = 7.

Table 1. Description of the conventional water extraction (CWE) and intensified water extraction (IWE) methods for ions extraction of soil water-soluble salts.

Extraction Methods	Water–Soil Ratio	Sieve Aperture	Main Reagents	Experimental Procedure	Measurement Methods
CWE	5:1	2 mm	H_2SO_4, $AgNO_3$, EDTA	The soil solution was shaken for 3 min at room temperature, filtered to obtain the leachate, and the content of each ion was determined immediately.	K^+, Na^+, Ca^{2+}, Mg^{2+} were determined by ICP-AES, and Cl^-, $SO_4{}^{2-}$, $HCO_3{}^-$, $CO_3{}^{2-}$ were determined by titration.
IWE	20:1	0.097 mm		The soil solution was shaken for 16 h at room temperature, centrifuged at 4500× *g* for 30 min, and the supernatant was measured immediately after passing through a 0.45 μm filter membrane.	

The determination of other indicators included the following: (1) passing the soil sample through a 2 mm sieve, and determining the filtrate pH using a Mettler–Toledo F2-Field portable pH meter and determining EC (ds m^{-1}) by a Mettler–Toledo conductivity meter (Mettler Toledo Technology Ltd., Shanghai, China), using a 5:1 water–soil ratio extraction [46]; (2) placing the soil sample that passed through a 0.2 mm sieve in a reaction bottle and determining the soil carbonate content by using the gasometric method [47]; (3) washing the soil sample that passed through a 0.25 mm sieve with 70% ethanol, thereby removing chloride salts and soluble sulfates, and then determining the gypsum content using the barium sulfate mass method [48,49]; and (4) determining the soil salt crystalline minerals using XRD (X-ray diffraction), while predominantly identifying calcite and gypsum. The detection process was conducted at the Xinjiang Mineral Experimental Research Institute using a Bruker D8 ADVANCE X-ray Diffractometer (Bruker Corporation, Karlsruhe, Germany), which utilized CuKα radiation (λ = 0.154 nm) at scanning angles of 2.5° to 52.0° (2θ) and a scanning step of 0.01° (2θ). And the basic information and characteristics of the sample soil are shown in Table 2.

Table 2. Basic information and soil characteristics of sampling sites in the study area.

Sample Number	Land Use History	Soil Texture	Soil Types	pH	EC (dS m^{-1})
30	Wheat fields irrigated by machine wells	Sandy soil	Desert–sierozem soils	7.93 *	0.70 *

* Representation of the average value.

2.4. Data Description and Processing

The pH values of the tested soils ranged from 7.65 to 8.41, with all the soil samples having no $CO_3{}^{2-}$ content. According to Lindsay [50], the $CO_3{}^{2-}$ content of the soil solution increases from 0 only when the soil pH exceeds 8.5. Therefore, $CO_3{}^{2-}$ was not detected in the results of both the CWE and IWE methods. The content of each water-soluble salt ion was measured in mg kg^{-1}; the total amount of soil salt content (g kg^{-1}) was calculated as the sum of the contents of K^+, Na^+, Ca^{2+}, Mg^{2+}, Cl^-, $SO_4{}^{2-}$, and $HCO_3{}^-$; and

the amount of carbonate determined by the gasometric method was reported as $CaCO_3$ (g kg^{-1}), while the gypsum determined by the barium sulfate mass method was expressed as $CaSO_4 \cdot 2H_2O$ (g kg^{-1}). The salt–crystalline minerals calcite and gypsum determined by XRD were expressed as Cal_{XRD} and Gy_{XRD}, respectively, and the values of both were relative percentages obtained by normalizing the peak intensities of their characteristic peaks.

SPSS 26.0 was used to perform a two-way ANOVA (analysis of variance) on the soil salinity ions (K^+, Na^+, Ca^{2+}, Mg^{2+}, Cl^-, SO_4^{2-}, and HCO_3^-) from different soil occurrence layers under the two extraction methods and a one-way ANOVA was performed for $CaCO_3$, $CaSO_4 \cdot 2H_2O$, Cal_{XRD}, and Gy_{XRD} under different tillage years. Duncan's test ($\alpha = 0.05$) was applied to these parameters to compare the differences between them. Data plotting was performed using Origin 2023b.

3. Results

3.1. Occurrence Layer Distribution of Salt Ions Extracted by the Two Extraction Methods

Figure 3 shows the distribution of each soil salt ion profile obtained using the two extraction methods. The contents of all the salt ions obtained by IWE leaching were higher than those obtained by the CWE method. In addition, in terms of the total salt content, the average total salt content obtained by the CWE and IWE methods was 2.52 and 14.68 g kg^{-1}, respectively, with the IWE result being 5.83 times higher (i.e., much higher) than the CWE result. In the extraction of water-soluble salts, increasing the water–soil ratio, oscillating time, and grinding to finer soil particles resulted in significantly higher extraction results for the salts from the desert–sierozem soil.

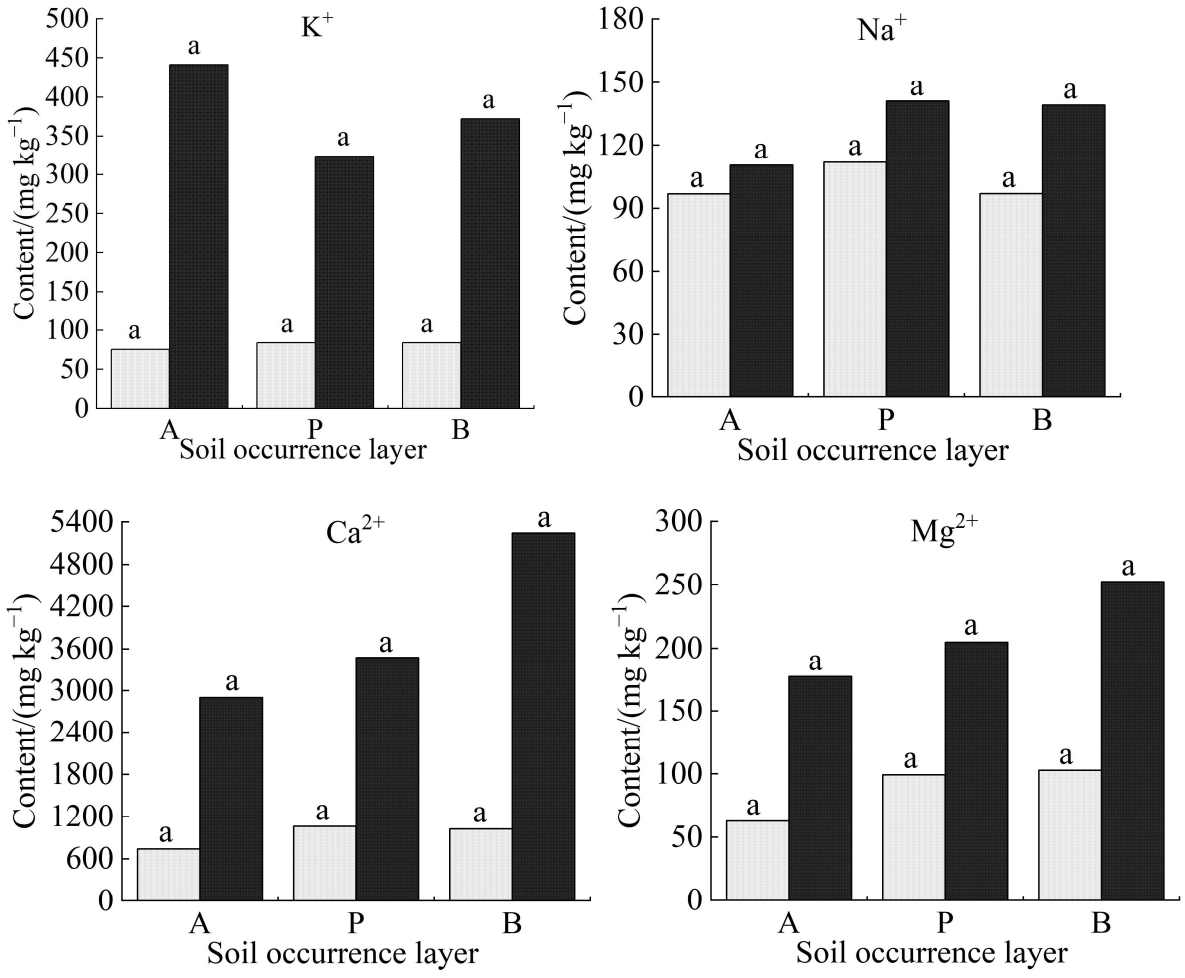

Figure 3. *Cont.*

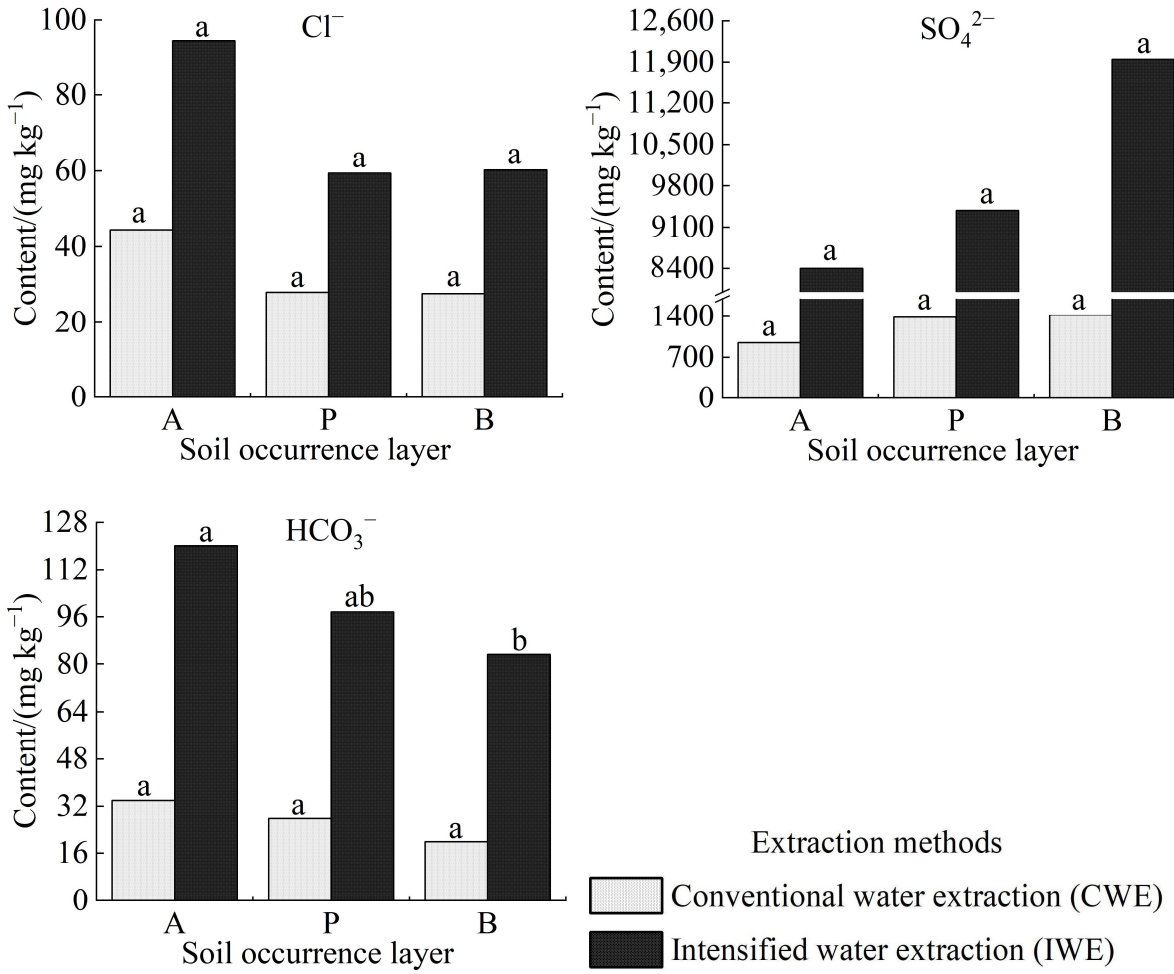

Figure 3. Distribution of salt ions in different soil layers under two extraction methods. Note: Different lowercase letters indicate differences between different soil occurrence layer for the same extraction method ($p < 0.05$).

As shown in Figure 3, none of the salt cations showed significant differences among the various occurrence layers when the same extraction method was used ($p > 0.05$). The content of the same ion determined by the CWE method did not differ significantly among the occurrence layers, whereas the content of different ions varied significantly. According to the CWE method, the average cation content followed the order $Ca^{2+} > Na^{+} > Mg^{2+} > K^{+}$. The Ca^{2+} cation proportions in the three layers A, P, and B were 61.80%, 67.30%, and 73.05%, respectively. The average cation content extracted by the IWE method followed the order $Ca^{2+} > K^{+} > Mg^{2+} > Na^{+}$, and the IWE-$Ca^{2+}$ content was much higher than those of the other three cations, with average cation proportions in the three layers A, P, and B of 55.77%, 66.32%, and 79.05%, respectively. The difference between the IWE-Na^{+} and CWE-Na^{+} contents was not significant, i.e., an average difference of 41.43 mg kg^{-1}, indicating that the CWE method could measure most of the Na^{+}. Conversely, there was a significant difference in the K^{+} content between the two extraction methods, with the IWE-K^{+} content being increased by 343.36 mg kg^{-1} on average compared with the CWE-K^{+} content. Mg^{2+} did not account for a significant cation proportion, with the IWE-Mg^{2+} content being increased by 123.41 mg kg^{-1} on average compared to the CWE-Mg^{2+} content. The average IWE-Ca^{2+} content was 3.82 times higher than the CWE-Ca^{2+} content, exhibiting an average increase of 2931.59 mg kg^{-1}, which was considerable. Based on the cation extraction results, both the CWE and IWE salts primarily consisted of calcium salts.

Upon comparing the results of the anion extraction from the two different methods (Figure 3), the IWE-Cl^{-} content was 2.56 times higher than the CWE-Cl^{-} content. Chloride

salts typically have high solubility and can be fully dissolved using the CWE method. However, experiments revealed a higher Cl^- content in the IWE method than that in the CWE method. This could be attributed to the larger sieve aperture of the soil samples, as specified in the extraction protocol of the CWE method, as well as the larger sample particles and a short shaking time, leading to incomplete dissolution of some chloride salts. The anion content in both extraction methods followed the order $SO_4^{2-} > HCO_3^- > Cl^-$, with SO_4^{2-} being the predominant anion. The average percentages of CWE-SO_4^{2-} in the three layers A, P, and B were 66.10%, 82.90%, and 85.87%, respectively. Likewise, the average percentages of IWE-SO_4^{2-} in the three layers A, P, and B were 71.73%, 78.27%, and 84.28%, respectively. The IWE-SO_4^{2-} content was 5.96 times higher than the CWE-SO_4^{2-} content, exhibiting an average increase of 8658.95 mg kg^{-1}. The anion extraction results indicated that sulfate was the primary salt present in both the CWE and IWE methods.

From the distribution of the salt ions in the different soil layers of the soil profile, it was found that the highest contents of Cl^- and HCO_3^- were in A layer, and the contents decreased with the increase in the soil depth, indicating the characteristics of surface accumulation, which were also in line with the characteristics of soluble salt, as they are more prone to move to the soil surface during the evaporation of soil water. The distribution of SO_4^{2-} in the profile was contrary to that of Cl^- and HCO_3^-, and its content increased with the depth of soil profile, i.e., B > P > A, which was similar to the distribution pattern of Ca^{2+} and Mg^{2+}, showing the characteristics of B layer precipitation. On the one hand, S is one of the essential nutrients for crops, and the SO_4^{2-} in layer A would be consumed by crop uptake. On the other hand, the solubility of calcium sulfate is lower than that of chloride salt and bicarbonate, and it is relatively not easy to move upward with the water during irrigation.

3.2. Salt Type Composition under the Two Extraction Methods

The anion contents are indicators of the salt types. According to the results obtained from the CWE method, 7.23% of the salt extracted was chloride, 78.29% was sulfate, and 14.48% was bicarbonate. Similarly, in the IWE method, 5.54% was chloride salt, 78.10% was sulfate salt, and 16.36% was bicarbonate salt. The two methods yielded similar soil salt types, with sulfate being dominant, bicarbonate being the second most prevalent, and chloride being the least prevalent.

Correlation analysis of salt ions can to some extent reveal the presence and composition of salt compounds. The salt ion data obtained using the two extraction methods were subjected to correlation analysis using a heat map, and the results are shown in Figure 4. In the CWE method, Cl^- showed highly significant positive correlations with K^+ and Na^+; however, these correlations were not revealed by the IWE method, likely due to the K^+ and Na^+ in the IWE method being obtained from leaching and attributed to soil colloid adsorption, which was exchanged into the solution during extraction, rather than all the release coming from chloride salts. As a result, the previous significant correlations were not observed in the IWE method. In both extraction methods, SO_4^{2-} showed highly significant positive correlations with K^+, Ca^{2+} and Mg^{2+}, while HCO_3^- showed highly significant negative correlations with Ca^{2+} and Mg^{2+}. The soil salts in the study area obtained by the CWE method were mainly chloride and sulfate salts, including KCl, NaCl, K_2SO_4, $CaSO_4$, and $MgSO_4$; meanwhile, the soil salts obtained by the IWE method were mainly sulfate salts, including $CaSO_4$, $MgSO_4$ and K_2SO_4.

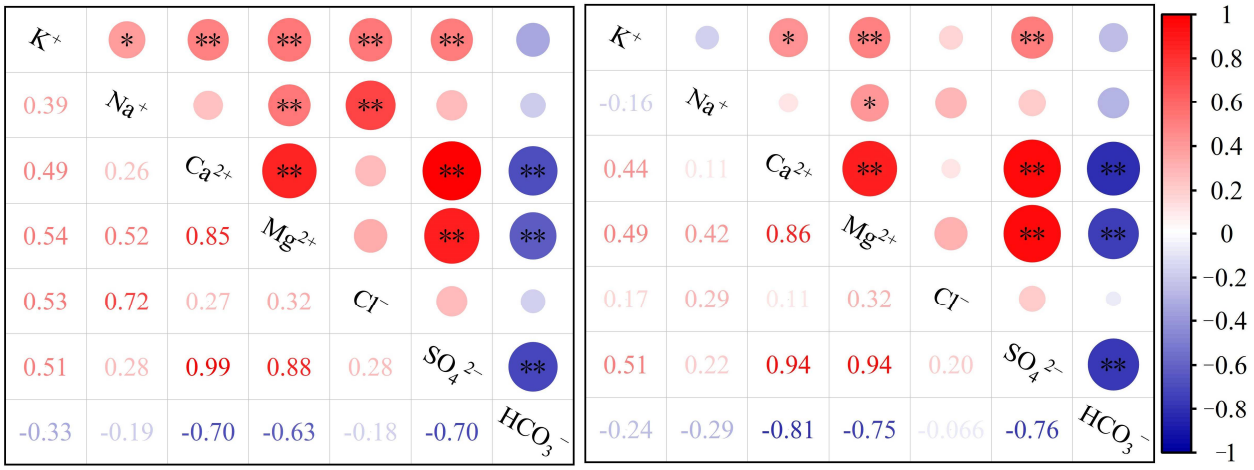

Figure 4. Correlation heat map of salt ions for the two extraction methods. Note: The positive and negative correlation coefficients in the correlation heat map represent the direction of the relationship (positive or negative correlation), while the size of the value represents the strength of the relationship. Color column in white represents 0, the closer to 1, the redder the color, the closer to −1, the bluer the color. * denotes significant correlation ($p < 0.05$), ** denotes highly significant correlation ($p < 0.01$).

3.3. Relationships between Water-Soluble Salt Ions and Calcium Sulfate and Calcium Carbonate

Desert–sierozem soils typically contain high amounts of calcium sulfate and calcium carbonate. This study employed chemical and physical methods to determine the non-crystalline and crystalline contents of these two calcium salts. Table 3 demonstrates the correlations between the salt ions and $CaCO_3$, $CaSO_4{\cdot}2H_2O$, Cal_{XRD}, and Gy_{XRD}. The analysis revealed no correlations of CWE-K^+ and CWE-Na^+ with the soil calcium carbonate and calcium sulfate, but it found highly significant positive correlations between IWE-K^+ and $CaSO_4{\cdot}2H_2O$. CWE-Ca^{2+}, IWE-Ca^{2+}, CWE-Mg^{2+}, and IWE-Mg^{2+}; CWE-$SO_4{}^{2-}$ and IWE-$SO_4{}^{2-}$ exhibited highly significant negative correlations with $CaCO_3$ and Cal_{XRD} and highly significant positive correlations with $CaSO_4{\cdot}2H_2O$ and Gy_{XRD}. $HCO_3{}^-$ had significant positive correlations with $CaCO_3$ and Cal_{XRD}, and highly significant negative correlations with $CaSO_4{\cdot}2H_2O$ and Gy_{XRD}. These results suggest that the Ca^{2+}, Mg^{2+}, and $SO_4{}^{2-}$ found in the leaching solutions of the CWE and IWE methods, as well as K^+ obtained from IWE leaching, originated from the dissolution of sulfates in the soil. The $HCO_3{}^-$ originated from the dissolution of carbonate.

Table 3. Correlation of the two extraction methods' ions with $CaCO_3$, $CaSO_4{\cdot}2H_2O$, Cal_{XRD} and Gy_{XRD}.

Experimental Indicators	$CaCO_3$	$CaSO_4{\cdot}2H_2O$	Cal_{XRD}	Gy_{XRD}
CWE-K^+	−0.234	0.267	−0.172	0.04
CWE-Na^+	0.076	0.235	0.045	0.085
CWE-Ca^{2+}	−0.697 ** [1]	0.790 **	−0.566 **	0.825 **
CWE-Mg^{2+}	−0.547 **	0.767 **	−0.493 **	0.650 **
CWE-Cl^-	−0.094	0.241	−0.040	−0.009
CWE-$SO_4{}^{2-}$	−0.718 **	0.798 **	−0.600 **	0.807 **
CWE-$HCO_3{}^-$	0.401 *	−0.611 **	0.419 *	−0.510 **
IWE-K^+	−0.237	0.466 **	−0.275	0.166
IWE-Na^+	0.073	0.265	−0.021	0.100
IWE-Ca^{2+}	−0.666 **	0.825 **	−0.573 **	0.693 **
IWE-Mg^{2+}	−0.631 **	0.897 **	−0.569 **	0.632 **
IWE-Cl^-	−0.118	0.320	−0.069	0.072
IWE-$SO_4{}^{2-}$	−0.736 **	0.909 **	−0.679 **	0.727 **
IWE-$HCO_3{}^-$	0.465 **	−0.716 **	0.446 *	−0.624 **

[1] * denotes significant correlation ($p < 0.05$), ** denotes highly significant correlation ($p < 0.01$).

3.4. Calcium Sulfate and SIC Sinks in Desert–Sierozem Soils of Different Tillage Years

Irrigation and tillage activities have altered the natural soil-forming environment and its processes. Table 4 shows the changes in the amounts of crystalline and non-crystalline calcium sulfate and calcium carbonate in the soils during different years of cultivation. This study discovered that the $CaCO_3$ content in desert–sierozem soils decreased initially and then increased over time with tillage. The highest level was observed at >40 years of tillage, with an average increase of 10.86 g kg^{-1} in $CaCO_3$ when compared to the level at 1–3 years of tillage; meanwhile, there was an increase of 2.22 g kg^{-1} in the crystalline mineral Cal_{XRD}. The $CaSO_4 \cdot 2H_2O$ and Gy_{XRD} contents initially exhibited increasing trends, followed by decreasing trends with increasing tillage duration. The maximum contents were observed after 10 years of tillage. However, at >40 years of tillage, the average $CaSO_4 \cdot 2H_2O$ content decreased by 13 g kg^{-1}, representing a reduction of nearly 80% compared to the case at 1–3 years of tillage. Conversely, the crystalline mineral Gy_{XRD} content decreased significantly to a point where it was no longer detectable using XRD.

Table 4. Distribution of inorganic salt and its salt–crystalline minerals in soils of different tillage years.

Tillage Year	1–3	10	20	30	>40
$CaCO_3$ (g kg^{-1})	67.62 ± 6.87 ab *	54.23 ± 23.57 b	69.02 ± 9.97 ab	71.32 ± 4.74 a	78.48 ± 8.21 a
$CaSO_4 \cdot 2H_2O$ (g kg^{-1})	16.40 ± 12.80 a	19.22 ± 12.93 a	13.67 ± 8.04 ab	7.57 ± 5.82 ab	3.40 ± 3.37 b
Cal_{XRD} (%)	3.77 ± 1.09 b	3.81 ± 2.46 b	5.39 ± 1.15 ab	5.73 ± 1.03 a	5.99 ± 0.99 a
Gy_{XRD} (%)	2.05 ± 2.03 ab	3.96 ± 4.66 a	2.13 ± 1.89 ab	0.64 ± 0.82 b	0 ± 0 b

* Different lowercase letters indicate significant differences among different years of tillage ($p < 0.05$).

4. Discussion

4.1. Salt Ion and Salt Composition in the CWE and IWE Methods

The K^+, Na^+, Ca^{2+}, Mg^{2+}, Cl^-, SO_4^{2-}, and HCO_3^- contents, which were determined using extraction methods with two different strengths of water-soluble salt ions, displayed relatively consistent distribution characteristics across the profile. Except for IWE-HCO_3^-, none of the ions showed significant variability among the soil layers using either the CWE or the IWE method. The K^+, Cl^-, and HCO_3^- contents were the highest in layer A, whereas Ca^{2+}, Mg^{2+}, and SO_4^{2-} were predominantly deposited in layer B, which was consistent with the findings of Wang et al. [51]. In comparison to the CWE method, the IWE method resulted in greater leaching amounts of K^+, Ca^{2+}, Mg^{2+}, SO_4^{2-}, and HCO_3^-, which was attributable not only to the soil particle size, water–soil ratio, and shaking time but also to the inherent natures of these ions. By comparing the changes in the K^+ and Na^+ contents extracted using the CWE and IWE methods, we discovered that the content and change range of IWE-K^+ were significantly greater than those of IWE-Na^+, which was due to the fact that both K^+ and Na^+ are easily soluble salt cations and migrate rapidly in soil. Nonetheless, the adsorption force, exchange force, and ionic cohesion of the soil colloids for K^+ are higher than those for Na^+ [52], accounting for the disparity between K^+ and Na^+. In addition, if the labile salt K_2SO_4 is present in the soil, it should be fully dissolved using the CWE method. Thus, the higher increase in IWE-K^+ compared to that in CWE-K^+ and its highly significant positive correlation with $CaSO_4 \cdot 2H_2O$ could be attributed to (1) a small amount of labile potassium salts in the CWE method that was not fully dissolved, (2) a notable increase in the adsorbed state of K on the soil colloids, as reported by Das et al. [53], that was subsequently desorbed into the soil solution during an extended period of shaking, and (3) the higher calcium content supporting soil potassium fixation, and according to Zou et al. [54], the application of calcium sulfate significantly improving the soil retention capacity for K^+ and reduced K^+ losses. Additionally, the IWE-Ca^{2+} content was much higher than the CWE-Ca^{2+} content, suggesting that the soils in the study region contained a large amount of calcium salts that were challenging to extract using the CWE method, and these calcium salts could be dissolved and leached out by intensifying the extraction process. Based on the anion extraction results presented in Figure 3, the anion contents

were dominated by SO_4^{2-}, followed by HCO_3^- and Cl^-, which was consistent with the results of Liu et al. [55], who investigated the soil salinity anion contents of cropland soils in an oasis.

In this study, we utilized the anion content percentage and correlations among the ions to identify the salt types, and the results showed that the two extraction methods indicated essentially similar salinity types. Consistent with the results of Luo et al. [56], SO_4^{2-} displayed highly significant positive correlations with K^+, Ca^{2+}, and Mg^{2+}, whereas HCO_3^- showed highly significant negative correlations with Ca^{2+} and Mg^{2+}. Based on the measured salt ion contents, the water-soluble salts in the soil from our sampling sites were dominated by sulfates, specifically moderately soluble calcium sulfate salts. In addition, the salts content extracted using the CWE method alone was significantly lower than the actual salt content in the soil. Notably, the CWE method extracted not only readily soluble salts, such as chloride salts, but also calcium sulfate salts from our samples.

Higher water–soil ratios, finer soil particle sizes, and longer oscillation periods were found to greatly increase the amounts of K^+, Ca^{2+}, Mg^{2+}, SO_4^{2-}, and HCO_3^- dissolved in the water. Therefore, the use of higher-intensity salt extraction methods is necessary to study the salinity levels, salt composition, and their changes in soils in arid zones, such as deserts and calcic soils. Further experiments are required to verify the universality of the appropriate extraction intensity for different soil types, which will provide a reference for the development of relevant experimental norms. Quantifying the forms and transformations of salts in the soil will improve our understanding of the soil material cycle in arid zones, which is crucial for scientific and rational soil development, amelioration, and utilization of oases, and for research on the impact of human activities on soil material cycling.

4.2. Involvement of Soil Calcium Sulfate in SIC Sequestration

The accumulation of SIC was closely related to the soil salinity and salt type in this study (Figure 5), and there was an highly significant linear negative correlation between the soil EC and $CaCO_3$ ($p < 0.01$), which was similar to the conclusion of Dong et al. [7]. The linear positive correlation between EC and $CaSO_4 \cdot 2H_2O$ also reached an extremely significant level ($p < 0.01$), and the R^2 was 0.633, indicating that the soil EC was mainly determined by sulfate in the study region.

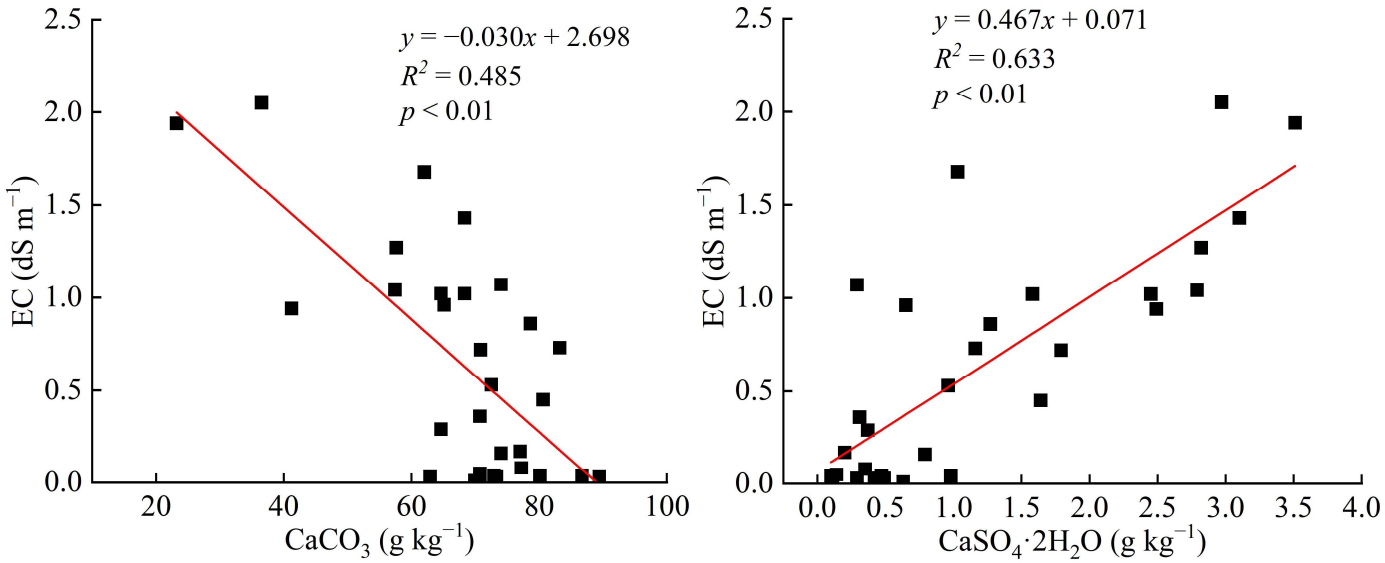

Figure 5. Fitted plot of EC to calcium carbonate and calcium sulphate.

There was a competitive relationship for Ca^{2+} between the calcium sulphate and calcium carbonate in the soil; therefore, the directions of their relationships with Ca^{2+} were opposite (Table 3). The Ca^{2+} in the leaching solution of our soil originated mainly from calcium sulfate or the dissolution of mineral gypsum; these Ca^{2+} reacted with the

C-containing anions (mainly HCO_3^-) in the soil [57,58] and participated in the microcarbon cycle of CO_2–HCO_3^-–SIC within the soil, which resulted in the formation of pedogenic carbonates. This was consistent with Li et al. [59], who found that Ca^{2+} and Mg^{2+} were the driving factors in the formation of inorganic carbon. Due to differences in water solubility, sufficient irrigation and the periodic alternating dry–wet process allowed for the transfer of calcium from sulfate to carbonate after plowing desert–sierozem soil in farmland. Thus, there was a highly significant negative correlation between calcium sulfate and calcium carbonate (Figure 6; $p < 0.01$). Of course, Mg^{2+} and Ca^{2+} have similar properties based on the measured salt ion contents, and the average Ca^{2+} content in desert–sierozem soil was over 10 times higher than that of Mg^{2+}; therefore, Ca^{2+} played a major role in the change in carbonate.

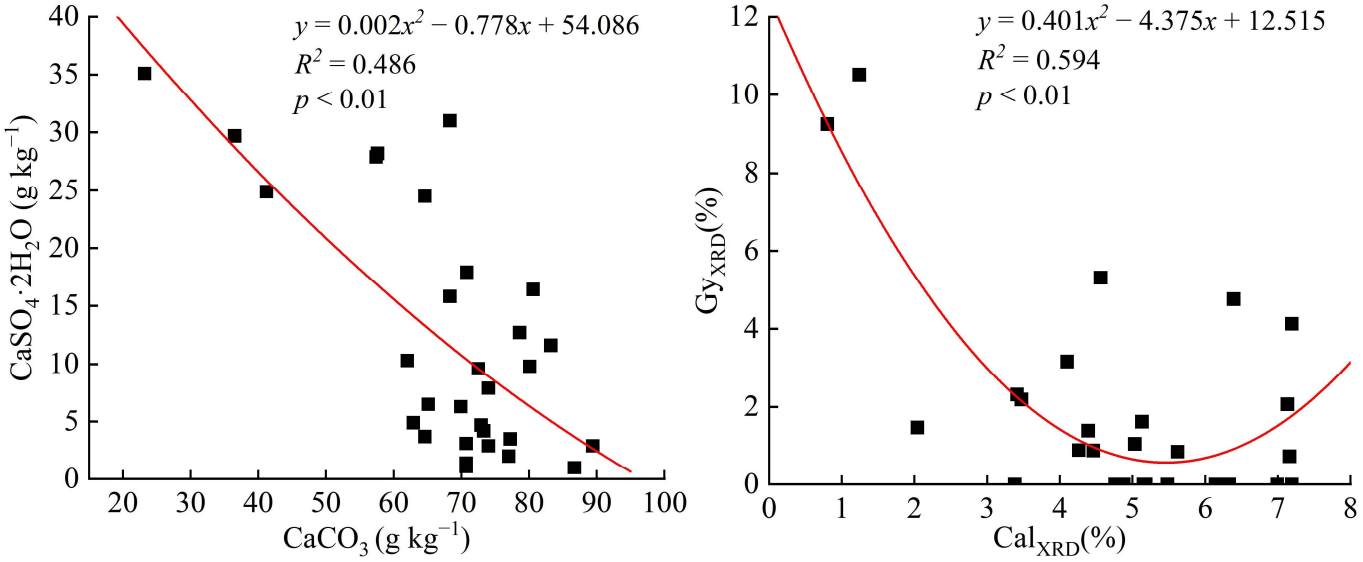

Figure 6. Fitted plot of calcium sulphate and calcium carbonate, calcite and gypsum.

Laudicina et al. [60] conducted a study on the net accumulation of inorganic carbon in semi-arid Mediterranean soils and confirmed that the calcium in gypsum played a role in the formation of soil carbon sinks. Our study further confirmed this process. Specifically, gypsum provides calcium ions for inorganic carbon formation, which involves the conversions of CO_2(g)–CO_2(aq)–HCO_3^-(aq)–$CaCO_3$(s) in the soil. Han and Tokunaga [61] confirmed that the presence of calcium sulfate enhanced carbon sequestration in weakly alkaline soils, and the soil samples collected in our study area had a pH ranging from 7.65 to 8.41, indicating a slightly alkaline range. Therefore, the substantial presence of gypsum in desert–sierozem soils could provide a material basis for pedogenic carbonate formation, leading to increased carbonate carbon sinks.

The inorganic carbon pool in arid zone soils is 2–5 times larger than the organic carbon pool, and its size is primarily represented by the soil calcium carbonate content [62]. The inorganic carbon pool in arid zone soils remains relatively stable during natural soil formation, and its change is very slow. Our study suggests that human tillage and irrigation activities likely accelerate changes in the SIC pool. After more than 20 years of cultivation, the $CaCO_3$ content in the soil was higher than its initial state and continued to increase, whereas the calcium sulfate content continued to decrease. This indicates that the elevated SIC in the desert–sierozem soil was capable of capturing contemporary atmospheric CO_2, and its potential to increase the SIC sink was linked to the Ca^{2+} supply capacity from non-carbonate sources. These Ca^{2+} can be derived from the transfer of other salts in the soil to carbonates or from irrigation water inputs [63]. In addition, silicate minerals, such as plagioclase, commonly found in arid zone soils are calcium-rich, and typically, the natural release of calcium from these minerals occurs slowly; however, soil maturation via cultivation can expedite the weathering process and release Ca^{2+} [64].

5. Conclusions

Soils in arid zones generally contain salt; therefore, it is important to use an appropriate salt extraction method to obtain the actual degree of salinity, salt types, and their changes. In this study, two water-soluble salt extraction methods with different extraction strengths, namely CWE and IWE, were used to extract salt ions from desert–sierozem soil. The results showed that the total salt content obtained by the IWE method was 5.83 times more than that obtained by the CWE method, and among all the ions, the cations were dominated by Ca^{2+} and the anions were dominated by $SO_4{}^{2-}$. The content of Ca^{2+} and $SO_4{}^{2-}$ increased with the soil profile depth, which was B > P > A, showing the characteristics of bottom accumulation. The salt types extracted using the two methods were similar and the sulfate content was greater than 78%. The results obtained from the two extraction methods differed considerably, and therefore, the extraction results from the IWE method provided more realistic soil salinity conditions in the study area. Desert–sierozem soils are well suited for agricultural exploitation, not only because sulfates provide important inorganic nutrients for crop growth but also because they help increase the soil carbon sequestration. As a kind of soil salt, the accumulation of SIC after tillage was closely related to the soil type, soil salt content, salt composition, and especially the supply of Ca^{2+} and Mg^{2+}. There are abundant calcium sulfate and calcium carbonate in desert–sierozem soils; after more than 40 years of cultivation, the $CaSO_4 \cdot 2H_2O$ content decreased by 13 g kg^{-1}, while the $CaCO_3$ content increased by 10.86 g kg^{-1} compared to their initial states, showing a strong carbon sequestrating potential. This potential was derived from the transfer of calcium released by calcium sulfate dissolution to secondary $CaCO_3$, which provided a material basis for the inorganic carbon pool of desert–sierozem soil to capture contemporary atmospheric CO_2.

Author Contributions: K.P. conceptualization, data curation, software, writing—original draft, writing—review and editing; F.Z. funding acquisition, investigation, writing—review, methodology, project administration, resources; Z.S. supervision, validation. All authors have read and agreed to the published version of the manuscript.

Funding: This work was supported by the National Natural Science Foundation of China (No. 41761041).

Data Availability Statement: The original contributions presented in the study are included in the article, further inquiries can be directed to the corresponding author.

Acknowledgments: We thank chief engineer Shi Yane for overseeing the experimental process.

Conflicts of Interest: The authors declare no conflicts of interest.

References

1. Xu, G.; Zheng, D.; Lu, D.; Guan, H.; Li, T. *General Catalogue of Chinese Geology-Soil Volume*; Shaanxi Normal University Publishing House: Xi'an, China, 2018; pp. 31–37.
2. Xinjiang Integrated Survey Team of the China Academy of Sciences. *Soil Geography of Xinjiang*; Science Press: Beijing, China, 1965; pp. 55–56, 149–164.
3. Cao, H.; Xie, J.; Hong, J.; Wang, X.; Hu, W. Organic matter fractions within macroaggregates in response to long-term fertilization in calcareous soil after reclamation. *J. Integr. Agric.* **2021**, *20*, 1636–1648. [CrossRef]
4. Zhang, F.; Xiong, H.; Feng, J.; Xu, Z. Changes in the carbon pool pattern and carbon pool migration during the expansion of new artificial oases in the northem fohills of Tianshan Mountains within the last 40 years. *Acta Ecol. Sin.* **2017**, *37*, 7862–7871. (In Chinese) [CrossRef]
5. Yang, W.; Jiao, Y.; Yang, M.; Wen, H.; Liu, L. Absorbed carbon dioxide in saline soil from northwest China. *Catena* **2021**, *207*, 105677. [CrossRef]
6. Haj-Amor, Z.; Araya, T.; Kim, D.G.; Bouri, S.; Lee, J.; Ghiloufi, W.; Yang, Y.; Kang, H.; Jhariya, M.K.; Banerjee, A.; et al. Soil salinity and its associated effects on soil microorganisms, greenhouse gas emissions, crop yield, biodiversity and desertification: A review. *Sci. Total Environ.* **2022**, *843*, 156946. [CrossRef] [PubMed]
7. Dong, X.; Wang, J.; Zhang, X.; Dang, H.; Singh, B.; Liu, X.; Sun, H. Long-term saline water irrigation decreased soil organic carbon and inorganic carbon contents. *Agric. Water Manag.* **2022**, *270*, 107760. [CrossRef]

8. He, B.; Ding, J.; Huang, W.; Ma, X. Spatiotemporal Variation and Future Predictions of Soil Salinization in the Werigan–Kuqa River Delta Oasis of China. *Sustainability* **2023**, *15*, 13996. [CrossRef]
9. Liu, G.; Tian, C.; Mai, W.; Azeem, A.; Yang, J. Spatial and Temporal Variation in Soil Salinity and Correlation with Groundwater Depth in the Karamay Irrigation District of China. *Sustainability* **2023**, *15*, 15680. [CrossRef]
10. Zamanian, K.; Pustovoytov, K.; Kuzyakov, Y. Pedogenic carbonates: Forms and formation processes. *Earth Sci. Rev.* **2016**, *157*, 1–17. [CrossRef]
11. Lan, Z.; Zhao, Y.; Zhang, J.; Jiao, R.; Khan, M.N.; Sial, T.A.; Si, B. Long-term vegetation restoration increases deep soil carbon storage in the Northern Loess Plateau. *Sci. Rep.* **2021**, *11*, 13758. [CrossRef]
12. Khalidy, R.; Arnaud, E.; Santos, R.M. Natural and Human-Induced Factors on the Accumulation and Migration of Pedogenic Carbonate in Soil: A Review. *Land* **2022**, *11*, 1448. [CrossRef]
13. Luo, Q.; Wang, Y.; Deng, C.; Niu, Z.; Li, Y. Dynamics of soil carbon storage under different land use years in arid agriculture. *Trans. Chin. Soc. Agric. Eng.* **2017**, *33*, 287–294. (In Chinese) [CrossRef]
14. Yan, A.; Wang, Z.; Jiang, P.; Weng, P. Effects of soil salinity on vertical distribution of soil carbon in saline soil in arid area. *Arid Zone Res.* **2017**, *34*, 770–774. (In Chinese) [CrossRef]
15. Lu, Q.; Wang, Y.; Li, Y.; Tang, L. A leaching experiment on inorganic carbon characteristics in the different soil salinity and irrigation in arid area. *Arid Land Geogr.* **2013**, *36*, 450–456. (In Chinese) [CrossRef]
16. Wang, X.; Xu, M.; Wang, J.; Zhang, W.; Yang, X.; Huang, S.; Liu, H. Fertilization enhancing carbon sequestration as carbonate in arid cropland: Assessments of long-term experiments in northern China. *Plant Soil* **2014**, *380*, 89–100. [CrossRef]
17. Zhao, W.; Zhang, R.; Huang, C.; Wang, B.; Cao, H.; Koopal, L.K.; Tan, W. Effect of different vegetation cover on the vertical distribution of soil organic and inorganic carbon in the Zhifanggou Watershed on the loess plateau. *Catena* **2016**, *139*, 191–198. [CrossRef]
18. Bayat, O.; Karimi, A.; Amundson, R. *Stable Isotope Geochemistry of Pedogenic Carbonates in Calcareous Materials, Iran: A Review and Synthesis*; Geological Society of London: London, UK, 2021; Volume 507, pp. 255–272. [CrossRef]
19. Hogg, T.J.; Henry, J.L. Comparison of 1:1 and 1:2 suspensions and extracts with the saturation extracts in estimating salinity in Saskatchewan. *Can. J. Soil Sci.* **1984**, *64*, 699–704. [CrossRef]
20. Aboukila, E.F.; Norton, J.B. Estimation of saturated soil paste salinity from soil-water extracts. *Soil Sci.* **2017**, *182*, 107–113. [CrossRef]
21. Ismayilov, A.I.; Mamedov, A.I.; Fujimaki, H.; Tsunekawa, A.; Levy, G.J. Soil Salinity Type Effects on the Relationship between the Electrical Conductivity and Salt Content for 1:5 Soil-to-Water Extract. *Sustainability* **2021**, *13*, 3395. [CrossRef]
22. Lu, L.; Li, S.; Gao, Y.; Ge, Y.; Zhang, Y. Analysis of the Characteristics and Cause Analysis of Soil Salt Space Based on the Basin Scale. *Appl. Sci.* **2022**, *12*, 9022. [CrossRef]
23. Feng, W.; Jiang, J.; Lin, L.; Wang, Y. Soil calcium prompts organic carbon accumulation after decadal saline-water irrigation in the Taklamakan desert. *J. Environ. Manag.* **2023**, *344*, 118421. [CrossRef]
24. Liu, X.; Yan, F.; Wu, L.; Zhang, F.; Yin, F.; Abdelghany, A.E.; Fan, J.; Xiao, C.; Li, J.; Li, Z. Leaching amount and timing modified the ionic composition of saline-alkaline soil and increased seed cotton yield under mulched drip irrigation. *Field Crops Res.* **2023**, *299*, 108988. [CrossRef]
25. Wang, R.; Wan, H.; Chen, S.; Xia, Y.; Bai, Q.; Peng, Z.; Shang, S. Spatial distribution pattern of soil salinization in farmland of Wulate sub-irrigation areas in Hetao Irrigation District in Inner Mongolia in spring. *Trans. Chin. Soc. Agric. Eng.* **2021**, *37*, 105–113. (In Chinese) [CrossRef]
26. Liu, S.; Cui, D.; Gu, J.; Liu, W.; Zhao, Y. The characteristics of soil salt ions under different diffusion stages of Sophora alopecuroides in the Yili River valley. *Chin. J. Ecol.* **2022**, *41*, 2137–2144. (In Chinese) [CrossRef]
27. Beijing Agricultural University. Measurement of soil water-soluble salts. *Chin. J. Soil Sci.* **1965**, *2*, 39–47. (In Chinese) [CrossRef]
28. Tang, S.; Liu, X.; Yang, K.; Guo, F.; Yang, Z.; Ma, H.; Liu, F.; Peng, M.; Li, K. Migration, transformation characteristics, and ecological risk evaluation of heavy metal fractions in cultivated soil profiles in a typical carbonate covered area. *Environ. Sci.* **2021**, *42*, 3913–3923. (In Chinese) [CrossRef]
29. Silva, B.P.C.; Silva, M.L.N.; Silva, S.H.G.; Silva, A.C.; Rocha, H.R.; Inda, A.V.; Mancini, M.; Curi, N. From rock to soil: Elemental mobility during pedogenesis in a deep Ultisol profile at the Mantiqueira Mountain Range, Southeastern Brazil. *Geoderma Reg.* **2022**, *31*, e00576. [CrossRef]
30. Tokalıoğlu, S.; Yılmaz, V.; Kartal, Ş. An assessment on metal sources by multivariate analysis and speciation of metals in soil samples using the BCR sequential extraction procedure. *Clean-Soil Air Water* **2010**, *38*, 713–718. [CrossRef]
31. Tessier, A.; Campbell, P.G.C.; Bisson, M. Sequential extraction procedure for the speciation of particulate trace metals. *Anal. Chem.* **1979**, *51*, 844–851. [CrossRef]
32. Sungur, A.; Soylak, M.; Yilmaz, S.; Özcan, H. Determination of heavy metals in sediments of the Ergene River by BCR sequential extraction method. *Environ. Earth Sci.* **2014**, *72*, 3293–3305. [CrossRef]
33. Gao, L.; Wang, Z.; Li, S.; Chen, J. Bioavailability and toxicity of trace metals (Cd, Cr, Cu, Ni, and Zn) in sediment cores from the Shima River, South China. *Chemosphere* **2018**, *192*, 31–42. [CrossRef]
34. Joon, N.K.; Ek, P.; Zevenhoven, M.; Hupa, L.; Miró, M.; Bobacka, J.; Lisak, G. On-line microcolumn-based dynamic leaching method for investigation of lead bioaccessibility in shooting range soils. *Chemosphere* **2020**, *256*, 127022. [CrossRef]

35. Mbodji, M.; Baskali-Bouregaa, N.; Barbier-Bessueille, F.; Ayouni-Derouiche, L.; Diop, C.; Fall, M.; Gilon, N. Speciation of metals by sequential extractions of agricultural soils located near a dumpsite for prediction of element availability to vegetables. *Talanta* **2022**, *244*, 123411. [CrossRef] [PubMed]
36. Tong, L.; He, J.; Wang, F.; Wang, Y.; Wang, L.; Tsang, D.C.W.; Hu, Q.; Hu, B.; Tang, Y. Evaluation of the BCR sequential extraction scheme for trace metal fractionation of alkaline municipal solid waste incineration fly ash. *Chemosphere* **2020**, *249*, 126115. [CrossRef]
37. Fuentes, A.; Lloréns, M.; Sáez, J.; Aguilar, M.I.; Ortuño, J.F.; Meseguer, V.F. Comparative study of six different sludges by sequential speciation of heavy metals. *Bioresour. Technol.* **2008**, *99*, 517–525. [CrossRef]
38. Hasan, M.; Kausar, D.; Akhter, G.; Shah, M.H. Evaluation of the mobility and pollution index of selected essential/toxic metals in paddy soil by sequential extraction method. *Ecotoxicol. Environ. Saf.* **2018**, *147*, 283–291. [CrossRef] [PubMed]
39. *GB/T 25282-2010*; Soil and Sediment—Sequential Extraction Procedure of Speciation of 13 Trace Elements. China Standards Press: Beijing, China, 2010.
40. Bao, S. *Analysis Methods for Soil Chemistry of Agriculture*, 3rd ed.; China Agriculture Press: Beijing, China, 2000; pp. 178–210.
41. Sun, J.; Xia, J.; Zhao, X.; Gao, F.; Zhao, W.; Xing, X.; Dong, M.; Chu, J. Enrichment of soil nutrients and salt ions with different salinities under Tamarix chinensis shrubs in the Yellow River Delta. *Catena* **2023**, *232*, 107433. [CrossRef]
42. Zhuang, Q.; Shao, Z.; Huang, X.; Zhang, Y.; Wu, W.; Feng, X.; Lv, X.; Ding, Q.; Cai, B.; Altan, O. Evolution of soil salinization under the background of landscape patterns in the irrigated northern slopes of Tianshan Mountains, Xinjiang, China. *Catena* **2021**, *206*, 105561. [CrossRef]
43. Du, Y.; Liu, X.; Zhang, L.; Zhou, W. Drip irrigation in agricultural saline-alkali land controls soil salinity and improves crop yield: Evidence from a global meta-analysis. *Sci. Total Environ.* **2023**, *880*, 163226. [CrossRef]
44. Filippi, P.; Cattle, S.R.; Pringle, M.J.; Bishop, T.F.A. A two-step modelling approach to map the occurrence and quantity of soil inorganic carbon. *Geoderma* **2020**, *371*, 114382. [CrossRef]
45. Chen, X.; Xiong, H.; Zhao, M. Response of the groundwater dynamic change based on C. W. Cobb-P. H. Douglas function model to the different crop yield and irrigation amount: A case study of well-based irrigation area in Qitai County in Xinjiang. *Res. Soil Water Conserv.* **2009**, *16*, 137–141. (In Chinese)
46. Rhoades, J.D. Cation exchange capacity. In *Methods of Soil Analysis*; Page, A.L., Miller, R.H., Keeney, D.R., Eds.; Part 2. Agronomy Monograph 9; American Society of Agronomy: Madison, WI, USA, 1982; pp. 149–157.
47. Loeppert, R.H.; Suarez, D.L. Carbonate and gypsum. In *Methods of Soil Analysis*; John Wiley & Sons Ltd.: Hoboken, NJ, USA, 1996; pp. 437–474.
48. Herrero, J.; Artieda, O.; Hudnall, W.H. Gypsum, a tricky material. *Soil Sci. Soc. Am. J.* **2009**, *73*, 1757–1763. [CrossRef]
49. Moret-Fernández, D.; Herrero, J. Effect of gypsum content on soil water retention. *J. Hydrol.* **2015**, *528*, 122–126. [CrossRef]
50. Lindsay, W.L. *Chemical Equilibria in Soils*; John Wiley & Sons: New York, NY, USA, 1979; pp. 87–103.
51. Wang, R.; Xu, C.; Liu, H.; Zhang, R.; Cheng, H.; Wang, Y. Spatio-temporal succession characteristics of saline-alkali soilprofile salt in Jingdian Irrigation District. *Agric. Res. Arid Areas* **2019**, *37*, 244–249. (In Chinese) [CrossRef]
52. Lv, Y.; Li, B. *Agrology*; China Agriculture Press: Beijing, China, 2006; pp. 100–114.
53. Das, D.; Dwivedi, B.S.; Datta, S.P.; Datta, S.C.; Meena, M.C.; Agarwal, B.K.; Shahi, D.K.; Singh, M.; Chakraborty, D.; Jaggi, S. Potassium supplying capacity of a red soil from eastern India after forty-two years of continuous cropping and fertilization. *Geoderma* **2019**, *341*, 76–92. [CrossRef]
54. Zou, L.; Fan, X.; Sun, Z.; Wang, J. Effects of desulfurized gypsum addition on saline- alkali soil nutrients and photosynthetic characteristics of cultivated oil-sunflower. *Chin. J. Appl. Environ. Biol.* **2012**, *18*, 575–581. (In Chinese) [CrossRef]
55. Liu, H.; Ding, B.; Bai, Y.; Zhang, J.; Wang, S.; Huang, Z. Spatial distribution characteristics of soil salinity in an oasis of typical arid regions in spring. *Chin. J. Soil Sci.* **2021**, *52*, 279–285. (In Chinese) [CrossRef]
56. Luo, Q.; Wang, Y.; Deng, C.; Ma, J. Distribution of inorganic carbon in soil profile and its relationship with soil saline-alkali property in arid area. *J. Soil Water Conserv.* **2017**, *31*, 240–246. (In Chinese) [CrossRef]
57. Su, P.; Wang, X.; Xie, T.; Wang, X.; Wang, L.; Zhou, Z.; Shi, R. Inorganic carbon sequestration capacity and soil carbon assimilation pathway of deserts in arid region. *Chin. Sci. Bull.* **2018**, *63*, 755–765. (In Chinese) [CrossRef]
58. Chen, B.; Feng, W.; Wang, Y.; Chen, Y.; Li, Y. Inorganic carbon sequestration effect of desulfurized gypsum in alkaline soil improvement. *Acta Pedol. Sin.* **2024**, *61*, 247–257. (In Chinese) [CrossRef]
59. Li, J.; Awasthi, M.K.; Zhu, Q.; Chen, X.; Wu, F.; Wu, F.; Tong, X. Modified soil physicochemical properties promoted sequestration of organic and inorganic carbon synergistically during revegetation in desertified land. *J. Environ. Chem. Eng.* **2021**, *9*, 106331. [CrossRef]
60. Laudicina, V.A.; Dazzi, C.; Delgado, A.; Barros, H.; Scalenghe, R. Relief and calcium from gypsum as key factors for net inorganic carbon accumulation in soils of a semiarid Mediterranean environment. *Geoderma* **2021**, *398*, 115115. [CrossRef]
61. Han, Y.S.; Tokunaga, T.K. Calculating carbon mass balance from unsaturated soil columns treated with $CaSO_4$-minerals: Test of soil carbon sequestration. *Chemosphere* **2014**, *117*, 87–93. [CrossRef]
62. Li, Y.; Wang, Y.; Tang, L. The effort to re-activate the inorganic carbon in soil. *Acta Pedol. Sin.* **2016**, *53*, 845–849. (In Chinese) [CrossRef]

63. Lei, M.; Zhou, J.; Wu, B.; Fan, W.; Zhang, J. Hydrogeochemical evolution process of groundwater in the eastern plains in Changji Hui Autonomous Prefecture, Xinjiang. *Arid Zone Res.* **2020**, *37*, 105–115. (In Chinese) [CrossRef]
64. Beerling, D.J.; Kantzas, E.P.; Lomas, M.R.; Wade, P.; Eufrasio, R.M.; Renforth, P.; Sarkar, B.; Andrews, M.G.; James, R.H.; Pearce, C.R.; et al. Potential for large-scale CO_2 removal via enhanced rock weathering with croplands. *Nature* **2020**, *583*, 242–248. [CrossRef]

Disclaimer/Publisher's Note: The statements, opinions and data contained in all publications are solely those of the individual author(s) and contributor(s) and not of MDPI and/or the editor(s). MDPI and/or the editor(s) disclaim responsibility for any injury to people or property resulting from any ideas, methods, instructions or products referred to in the content.